Available online at www.sciencedirect.com

ScienceDirect

journal homepage: www.elsevier.com/locate/he

PTFE mapping in gas diffusion media for PEMFCs using fluorescence microscopy

Nicholas McCarthy [a], Rui Chen [a,*], Gregory Offer [b], Robert Thring [a]

[a] Department of Aeronautical and Automotive Engineering, Loughborough University, Loughborough, LE11 3TU, UK
[b] Department of Mechanical Engineering, South Kensington Campus Imperial College London, London, SW7 2AZ, UK

ARTICLE INFO

Article history:
Received 4 May 2016
Received in revised form
26 July 2016
Accepted 31 July 2016
Available online 20 August 2016

Keywords:
Fuel cell
MEA
PTFE
Microscopy
Fluorescence
GDL

ABSTRACT

Differentiating between the various polytetrafluoroethylene based structures inside polymer electrolyte membrane fuel cells with a degree of certainty is necessary to optimize manufacturing processes and to investigate possible degradation mechanisms. We have developed a novel method using fluorescence microscopy for distinguishing the origin and location of PTFE and/or Nafion® in Membrane Electrode assemblies and the gas diffusion media from different sources and stages of processing. Fluorescent material was successfully diffused into the PTFE based structures in the GDM by addition to the 'ink' precursor for both the microporous layer and the catalyst layer; this made it possible to map separately both layers in a way that has not been reported before. It was found that hot pressing of membrane coated structures resulted in physical dispersion of those layers away from the membrane into the GDM itself. This fluorescence technique should be of interest to membrane electrode assembly manufacturers and fuel cell developers and could be used to track the degradation of different PTFE structures independently in the future.

Introduction

Polytetrafluoroethylene (PTFE) based polymers play several important roles in polymer electrolyte membrane fuel cells (PEMFCs). A sulphonated variant is the backbone of the most commonly used solid electrolyte in the form of Nafion® membranes. PTFE based polymers are also used as hydrophobic coatings on carbon fibers, binder agents for catalyst layer (CL) inks, to provide structural integrity for microporous layers (MPL) and as an adhesive binder for the various layers that form the final membrane electrode assembly (MEA). By using PTFE based polymers for these differing functions, improved adhesion between the various structures is promoted by their broadly similar chemistry. For some types of MEAs the various coatings and functional layers are applied directly to the membrane, and in others the coatings are applied to the gas diffusion media (GDM) adjacent to the membrane. These are generally applied as a liquid suspension, and the impregnation of these PTFE solutions into the GDM make a significant impact on the final porosity of the completed MEA.

The hydrophobicity (water contact angle) of GDMs has been commented on and studied extensively by a wide array

* Corresponding author.
E-mail addresses: n.mccarthy@lboro.ac.uk (N. McCarthy), r.chen@lboro.ac.uk (R. Chen), gregory.offer@imperial.ac.uk (G. Offer), R.H.Thring@lboro.ac.uk (R. Thring).

http://dx.doi.org/10.1016/j.ijhydene.2016.07.270

of authors [1–5], who all agree that the coatings applied, to modify the hydrophobicity of the GDM, is an important factor in determining its overall performance of the fuel cell. Comprehensive reviews of this topic [6] and other GDM issues [7] agree that water contact angle has a significant impact on the fuel cell performance. Typically the control of the wetting angle on the carbon fibers is achieved by the addition of a PTFE based polymers to the carbon fibers during the manufacture of the GDM, and in some cases this coating is an important part of the GDM fabrication method, binding together non-woven structures. In other cases the hydrophobic polymer content is added solely to change the water transport properties of the GDM. This additional polymer coating is, like many engineering solutions, a compromise between increased hydrophobicity to facilitate water transport and a decrease in the available pore volume for fluid transport in the GDM.

When it comes to the fundamental understanding of reactant and product mass transport mechanisms in the fuel cell, the through plane thickness, total volume or percentage surface coverage of these various layers can be a significant consideration. Typically an examination of 'Spatially-Varying' performance of fuel cells will consider the MEA as a plane. These studies seek to understand localized performance variations across the plane of the MEA, usually as a result of reactant and product concentration changes, along the length of the gas flow channels [8–10]. Some work in this area has investigated the variation in the fuel cell through the plane of the MEA [11], focusing on the distribution of water through the plane of the GDM; not the direct measurement of PTFE structures through the plane of the GDM.

For example, in agglomerate models of catalyst layers an estimation of the thickness of CL is a key factor. This is often done by determining the total mass of catalyst material applied, and then assuming a uniform, monolayer distribution. For layered catalyst structures this estimation is done iteratively for each subsequent level [12,13]. For the catalyst coated substrate (CCS) manufacturing method – where the CL is applied to the GDM and not the membrane – this is also used. However, the validity of this through plane thickness assumption becomes questionable as mass gain is no longer an accurate indication of the dimensions of each layer applied to the complex, porous surface of the carbon fiber GDM. This same principle applies to other PTFE based surface treatments such as the addition of microporous layers. In many cases these PTFE based layers, and their exact dimensions, cannot be defined with any certainty when the GDM has been pretreated with a hydrophobic (PTFE based) coating. Energy Dispersive X-ray (EDX, or 'EDaX') techniques and secondary backscatter electron imaging have all been used in conjunction with Scanning Electron Microscopy to map various chemical species in the MEA [14]. Heavier atomic weight molecules and atoms show up as a brighter contrast to lighter species in the standard image with the induced emission of x-rays (of a specific energy and frequency) being used to identify the individual chemical species. This makes chemical species that are largely composed of carbon difficult to distinguish between. It is this brightness value and species identity that is used to generate chemical composition maps such as those in Fig. 1(c) where the Fluorine response has been highlighted in red, and to distinguish it from the other adjacent carbon based structures. For a comparison between the graphitized carbon fibers of a typical GDM, and the largely carbon based PTFE species present in the system, fluorine detection is typically recommended. The limitation of this technique is that it is impossible to distinguish the fluorine content of two different PTFE sources. For example if a MPL layer has a PTFE based dispersive agent, and the catalyst ink is applied with a 10wt% solution aqueous Nafion solution, both will give an equal response in fluorine mapping with EDX analysis. Fig. 1 (c & d) show a typical fluorine map generated from EDX. As can be clearly seen there is no way to numerically differentiate the fluorine in the image between the various PTFE based polymers (ink, MPL, CL and hydrophobic coatings on fibers) in the MEA that generate a fluorine response.

In the case where SEM/EDX mapping of the MPL layer was desirable, a low concentration of 10 weight percent of platinum on carbon (10wt% Pt-on-C) can be deposited in the same way as an MPL. This low concentration of heavy metals is an attempt to differentiate between various layers of the MEA. This is reliant on the assumptions that the platinum doped carbon particles are uniformly spread through region of interest, and that the PTFE based polymers used in the MPL 'ink' are dispersed throughout the material in the same way. This 'functionalized' MPL is equivalent to the dual layer catalyst systems suggested by some researchers [15–18], and according to their finding it must be acknowledged that fuel cell performance is changed by this approach. Furthermore by taking this approach we have now in turn made it impossible to clearly differentiate between the MPL and CL. Additionally this low concentration of Platinum approach cannot be used at the same time for other PTFE structures in the MEA such as the PTFE based hydrophobic coatings, especially for comparisons with standard GDMs used in fuel cell research. There has been a great deal of work using novel imaging techniques such as X-ray tomography (XRT) to aid the conceptualization of the internal structures of the GDM and its impact on the performance of performance of fuel cells [19,20]. Synchrotron or neutron based imaging techniques can also be used to visualize the water generation and flow inside a working fuel cell in real time [21–24]. These processes require specialist equipment, and in the case of XRT a significant level of expertise and computer processing time to process the captured images. Whist these techniques can demonstrate the overall impact of water flow (neutron imaging), or identify the totality of the combined structure of fibers and PTFE additions (XRT); both suffer the same limitations as EDX and cannot differentiate between multiple sources of PTFE content in the GDM.

An alternate methodology is needed for mapping the distribution of these various layers and coatings in the MEA. A system that will not change the performance of the MEA under operating conditions would obviously be preferred. With this in mind the following work was undertaken to determine if fluorescence based microscopy could be used to differentiate between different polymeric materials within the GDM; with the intention that this can be used to optimize GDM/PTFE interactions. In this paper we present the use of a fluorescent dye doped directly into the PTFE component of a layer of interest, and map the PTFE distribution in a CL and MPL separately in multiple MEAs.

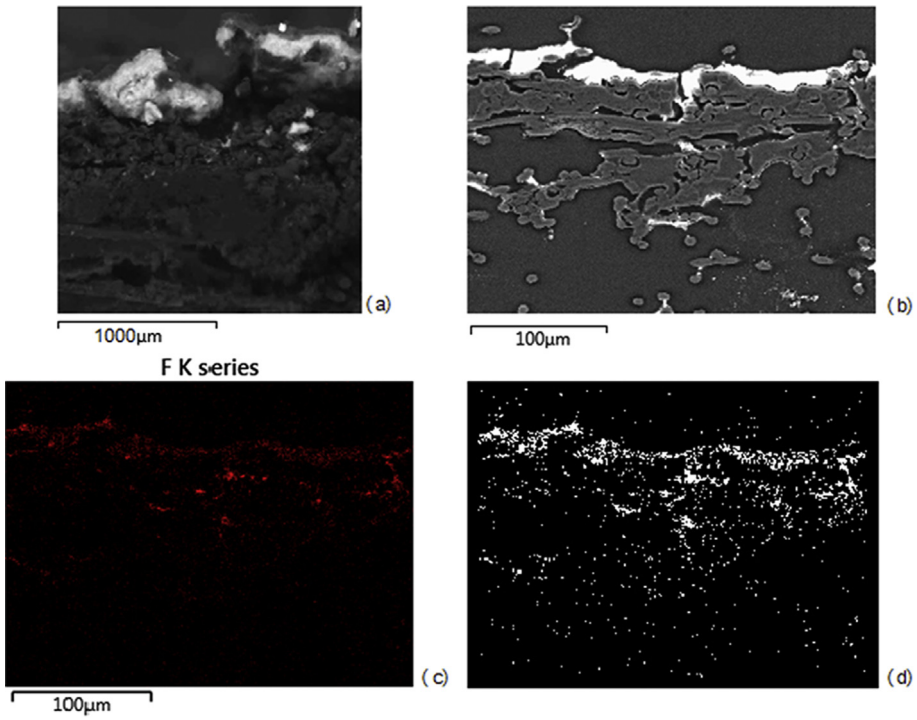

Fig. 1 – SEM of standard cathode GDM (a) optical image, (b) SEM image, (c) Back scatter map of Fluorine, Black and White processing of 'c' (d).

Litster et al. [25] in 2006 utilized fluorescent water impregnation to characterize the liquid penetration time through GDM and also to gain greater understanding of the pathways for water penetration through the material. Their work provided the inspiration for this work to consider the possibility of faster and more cost effective ways of assessing the PTFE distributions in the GDM in the CL and MPL. To date there has been no work done to assess the interaction of catalyst ink formulations and their impact on PTFE distributions in the GDM or CCS type fuel cell assemblies. This is due to the inability of SEM/EDX techniques in generating clear separation of the elemental species in the carbon based fibers, the carbon based catalyst inks, the carbon (PTFE) based GDM binder agents and the Carbon (PTFE) based catalyst ink suspensions. This inability to distinguish chemically similar phases in a sample is not unique to the field of fuel cells. Fluorescence in degradation products is well known in the food sciences, yet they are often difficult to distinguish for different stages of the ripening/decomposition process. As highlighted by Croptova et al. [26] it is possible to correlate with a high degree of confidence (95% confidence level easily achieved in their study) the emitted fluorescence of a single phase of interest in a chemically complex system, especially if the filter system used in the experimental set up is optimized. Le Duigou et al. [27] have also used fluorescence microscopy to differentiate between optically similar samples in their confocal microscopy analysis; mapping resin impregnation into the fibrous structures of an epoxy-flax composite. This is a very similar environment to the PTFE impregnated carbon fibers for the GDM. Whittman et al. [28] examined the impact of organic fluorescent dye on PTFE type materials, and indicated that, with the correct heat treatment regime, the fluorescent dye can alter the structure of the PTFE materials, and form a PTFE/copolymer composite material. This provides solid evidence that the proposed concept – that a fluorescent dye will mix with the PTFE component of a catalyst ink formulation and make it possible to track its distribution through the GDM – is worthy of further investigation.

Experimental

Five fluorescent dye concentrations were investigated. Concentrations between 0.5 and 10 wt% of EpoDye™ added prior to sonication of the ink formulation in each case. EpoDye™ is a propriety brand of 'Brilliant yellow 43' ($C_{20}H_{24}N_2O_2$), which typically has its highest stimulation frequencies in the 275 nm–450 nm wavelengths, comfortably in the Ultraviolet spectrum and so well suited to fluorescence microscopy with mercury lamp illumination. The use of 2-propanol in the ink formulation described in this paper indicates this solvent dye should be suitable. The 1wt% EpoDye™ loading was found to achieve the maximum luminescent response with the least amount of material added, and was in line with the manufacturers recommended dosing levels. The 0.5wt% doped fluorescent samples (Fig. 2 (b)) could, after a prolonged exposure time, generate a usable image, and were very well suited to generating sufficient contrast to examine the fiber structure of the GDM. Higher weight percentages generated a more complete coverage of the GDM surface as shown in figures (c & d).

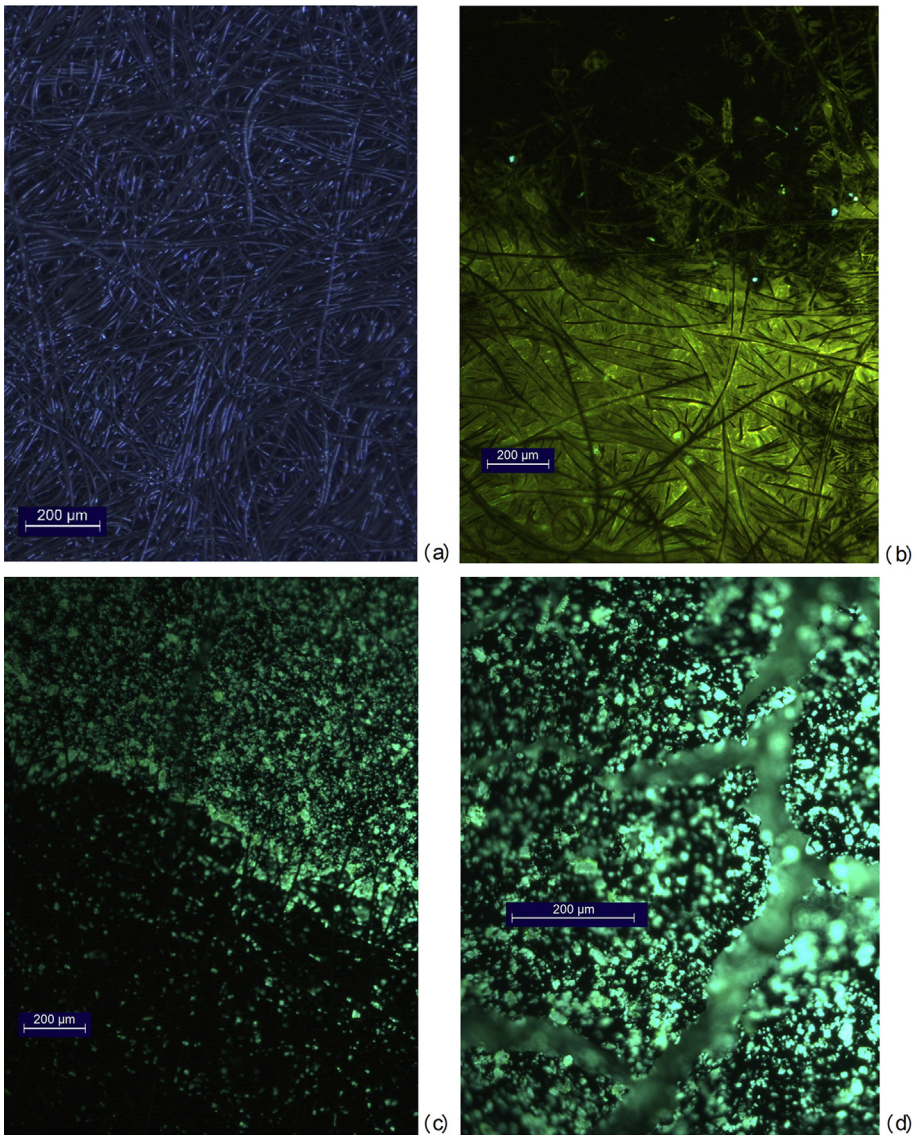

Fig. 2 – (a) Auto-fluorescence of cathode carbon fibers, (b) 0.5wt% EpoDye™ doped cathode carbon fibers, (c) 1.0wt% EpoDye™ doped cathode carbon fibers, (d) 400× magnification image of Microporous layer structure.

Catalyst ink formulations

Various ink formulations in the literature [29–31] were adapted until a stable ink manufacturing procedure was developed. DI water, and 30 'weight percent' (30wt%) of platinum (Pt) on carbon (C)[1] and 10wt% aqueous Nafion® solution, and 1 M 2-propanol solution (IPA) are sonicated together for 1 h. To determine the total amount of aqueous Nafion® solution required (in μL) for the ink; the mass of carbon desired (catalyst weight not included) in mg is divided by the percentage Nafion solution strength (expressed as a decimal).

$$Nafion_{soln.}(\mu l) = \frac{m_{Carbon}(mg)}{\%_{soln.}(asdecimal)} \quad (1)$$

5.31 times this value derived in Eq. (1) gives the volume of 2-propanol required

DI water with a volume equal to 10% of the measured out volume of 2-propanol (isopropanol) is first added to the Pt on C to reduce the possibility of combustion during mixing. The whole mixture is then sonicated at room temperature for one hour immediately before application. Single layers of ink are painted on, and then allowed to dry for eight hours (or overnight). The MEAs are weighed, and the process repeated until the desired catalyst loading is achieved. The ink preparation is sonicated for twenty minutes immediately prior to application if it has been left static for a significant period of time (more than three hours).

MPL equivalent inks were manufactured in much the same way, but with carbon particles with no platinum, or in the case where EDX mapping of the MPL dimensions was required with a 10wt% Pt-on-C loading.

[1] Carbon black catalyst support was 'Vulcan carbon black' according to the suppliers.

Fluorescent dye study

Due to the lack of contrast between the carbon based ink and the carbon fiber support; typical optical microscopy of the CCS active surface results in a more or less uniform 'black field' image that has little or no discernible features that can be effectively imaged. Non-woven fibers with a hydrophobic coating and without carbon based ink coatings could, with extremely long exposure times under UV light, induce any PTFE present to emit characteristic auto fluorescence (Fig. 2 (a)). All microscopy images were captured using a Leica DMRX fluorescent microscope equipped with a Leica DFC480 5 Mega pixel digital color camera. Surface images of MEAs with fluorescent dye doped inks demonstrate a characteristic 'green' color (Fig. 2 (b,c &d)) as a result of the use of a violet/blue filter cube: an 'E4' band pass filter from Leica. This reduces the overall intensity of the light emitted, but also reduces the signal to noise ratio by filtering out much of the visible light except for the 436/7 nm wavelength, and a proportion of those frequencies at or above 513 nm. This can be used beneficially to image the mixed blue light (436/7 nm) with the yellow/green light emitted from the EpoDye™ in solution with the PTFE in the ink: Making it possible to differentiate between the yellow florescence of the doped PTFE component in the catalyst ink and the naturally 'blue' fluorescence of the (untreated, PTFE based) binder agents, the phobicity controlling surface treatments of the GDM itself.

Having completed the conditioning and initial polarization curves, samples were edge mounted and cross sectioned for microscopy. In order to maintain the GDM structure great care was taken over the polishing procedure, as it was found more aggressive polishing recipes resulted in fiber pull out and disrupted the GDM structure. To maintain GDM structural integrity in the polishing stage, all samples were mounted in low viscosity epoxy resin (EpoFix™) and vacuum impregnation was used to support the carbon fibers during the polishing process. The resin was then left to set for 24 h and polishing of samples for optical microscopy was carried out.

MEA fabrication and test cell dimensions

The fabricated MEAs active surface area is 11.34 cm^2. Graphite current collection plates are used, with a single serpentine circular ('disc-like') flow field. The GDM anode material was Toray TGP-H-120 with a catalyst loading of 0.3 mg cm^{-2} (±0.02 mg cm^{-2}). The cathode material was much the same with 0.35 mg cm^{-2} (±0.02 mg cm^{-2}) of catalyst. Nafion 212 Polymer Electrolyte Membranes (PEMs) are used. The electrodes and the membrane are hot pressed at 125^{O}C and 1.0 MPa for two minutes.

Two sets of MEA were fabricated. In order to analyze not only the applicability of the fluorescence technique, but to also determine how small a resolution of the PTFE distribution could be effectively analyzed; a mixed application cathode (MAC) manufacturing technique was used. A high Pt concentration layer (40wt% Pt-on-C) was deposited directly onto the membrane in one layer, and a low concentration (10wt% Pt-on-C) was deposited directly onto the GDM in another layer. This lower concentration layer acting as the effective MPL, but with additional heavy metal in the hopes of aiding SEM image capture at a later stage.

These two mixed application catalyst samples were identified as MAC1 and MAC2. In MAC1 the fluorescent dye is in the catalyst layer, and in 'MAC2' it is the MPL that has been doped with fluorescent dye. In this way we hope to see what the minimum resolution of this technique could be. Recall in this work the layer furthest away from the membrane is the low concentration platinum layer and can be considered as a MPL rather than as a true CL.

Having determined the mass loading for each layer as described previously, the ink solutions were hand painted on. The MEA was then fabricated up in the usual way. MAC1 has 1wt% EpoDye™ on the membrane side of the MAC assembly. Mac 2 has 1wt% EpoDye™ on the GDM side of the assembly.

Polarization performance

Having established the feasibility of the approach, MEAs were fabricated and tested under operational conditions. All MEAs were conditioned at 0.6 V (+/−0.05 V) for three hours at 60 °C. Twenty polarization curves were then run on each sample. After this conditioning cycle was completed an additional set of polarizing curves were undertaken. All samples were tested at 65 °C (+/−2 °C) at 100% relative humidity with a hydrogen flow rate of 60sccm and an air flow rate of 150sccm. All gases were at 150 kPa absolute and the fuel cell clamping assembly was tightened down to 2Nm of torque per bolt on a three bolt system (circular geometry). The test apparatus is a 'self −humidifying' system that does not make use of pre-humidified or pre-heated reactant gas streams. Such self-humidifying systems result in an anticipated reduction in the overall performance [32] of the cell when compared to pre-humidified and pre-heated gas stream results.

The performance of the EpoDye™ doped fuel cells was very poor, indicating the dye inhibits the system. For the 'MAC2' sample getting any sort of polarization curve at all took several attempts, and the conditioning regime had to use a significantly reduced load to achieve the twenty 'conditioning' polarization curves. A comparative MEA without fluorescent dye (un-doped) is also shown (Fig. 3) labeled as control.

Results & discussion

SEM and EDX study

Images in Fig. 1 were taken with a Cambridge Instruments Stereoscan 360 Tungsten Filament SEM. In Fig. 1(b) the standard SEM image of a prepared GDM in cross section can be seen. The lighter, brighter section in the grey scale image represents heavier atomic mass elements. EDX was used to generate the map shown in Fig. 1(c). However, as shown in Fig. 1(d) the ability of the technique to map the distribution of the fluorine molecules (the only way to differentiate the PTFE based Nafion® from the remaining carbon based structures) is extremely limited. The F k series response in Fig. 1(d), gives no clear demarcation between the various layers. Numeric assessment of the two separate PTFE layers (MPL and CL) in this sample was impossible when based on Fluorine

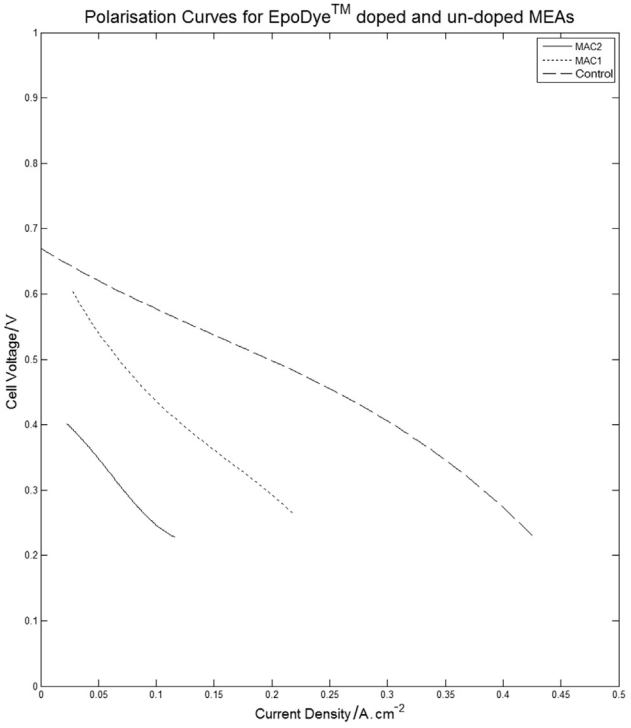

Fig. 3 – Polarization response of MEAs with and without fluorescent dye.

distribution only. When examining a GDM that has been pre-treated with a hydrophobic layer, the ability to distinguish PTFE based layers through fluorine molecule mapping becomes indeterminable (Fig. 1(c)).

In order to process such images the threshold has to be 'turned up' to the point where when running a standard image analysis tests (using MatLab®) the simplified black and white image as shown in Figs. 1(d) and 4(a) is produced. In this case the threshold level used to decide if a given pixel should be converted to 'black' or 'white' is set at 50% of the total brightness of all pixels in the equivalent grayscale image. Fig. 4(a) shows two distinct regions of PTFE distribution, with the histogram (Fig. 4(b)) showing the centroid point of each discrete point mapped. Therefore it is not possible to answer the question: has the CL or MPL added to this GDM actually penetrated ~200 μm into the body of the GDM, or has the image processing software incorrectly identified the pre-existing hydrophobic coating in the GDM fibers instead? Traditional EDX cannot answer this question.

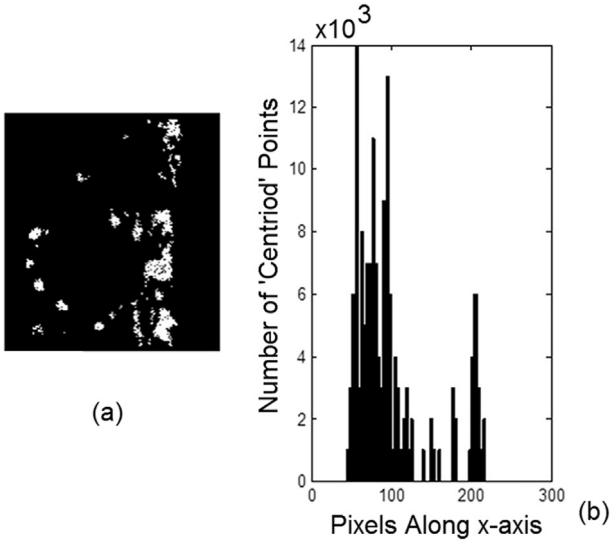

Fig. 4 – (a) Black and white processed image of standard GDM cathode Fluorine content, (b) 'centroid point' locations of individual particles in 'a'.

As stated previously, a low Pt loading system is used to help identify through scanning electron microscopy (SEM/EDX) the likely distribution of the MPL. Comparison to Fig. 1(d) the fluorine response is far superior in mapping the distribution of the PTFE based MPL, and the addition of a small amount of Platinum is needed to define the boundaries of the MPL itself.

Fluorescent dye study

Fig. 2(a) shows an 'as received' GDM material yet to be coated with catalyst ink. Note the light blue highlights as a result of the inherent PTFE based hydrophobic coating in the GDM fluorescing as is common for many organic molecules ("*auto-fluorescence*" [33]). The time taken to create this image was extremely long; well in excess of 60 s. This is impractical for the significant numbers of pictures used in large scale imaging studies and automated quality control in mass production lines. The fluorescent image could only be generated at 100× magnification or greater. This reduces the field of view for the surface of the GDM, and would again limit the utility for catalyst optimization studies for larger surface area GDMs. This long exposure time increases significantly the excitation of fluorophores that are out of focus (beyond the depth of field of the captured image as detailed in Table 1). Therefore whilst the image contrast is increased by increased exposure times, the amount of in–focus information is not increased at the same rate and excess exposure can reduce the overall value of a given fluorescent image. Therefore additional fluorescent material is required to reduce the exposure time, and improve image capture at lower magnifications.

It was found that at higher magnifications it was possible to view the open structure of the MPL itself (note that in image Fig. 2(d) the MPL has been dried overnight and the full development of MPL structure as a result of hot pressing is not represented here). Prior to MEA assembly, sample sections of GDM were coated with the fluorescent catalyst ink, and it proved possible to examine the CCS active surface in excellent detail.

In the cross section (Fig. 5) of the same GDM in Fig. 1(a) we clearly see florescence from the untreated PTFE binders, and

Table 1 – Depth of field at various magnifications.

Total magnification through camera	50×	100×	400×
Numeric Aperture (NA)	0.15	0.30	0.75
Focal Lens	5×	10×	40×
Depth of field (UV light source mean λ = 350 nm)	15.5/μm	3.9/μm	0.6/μm

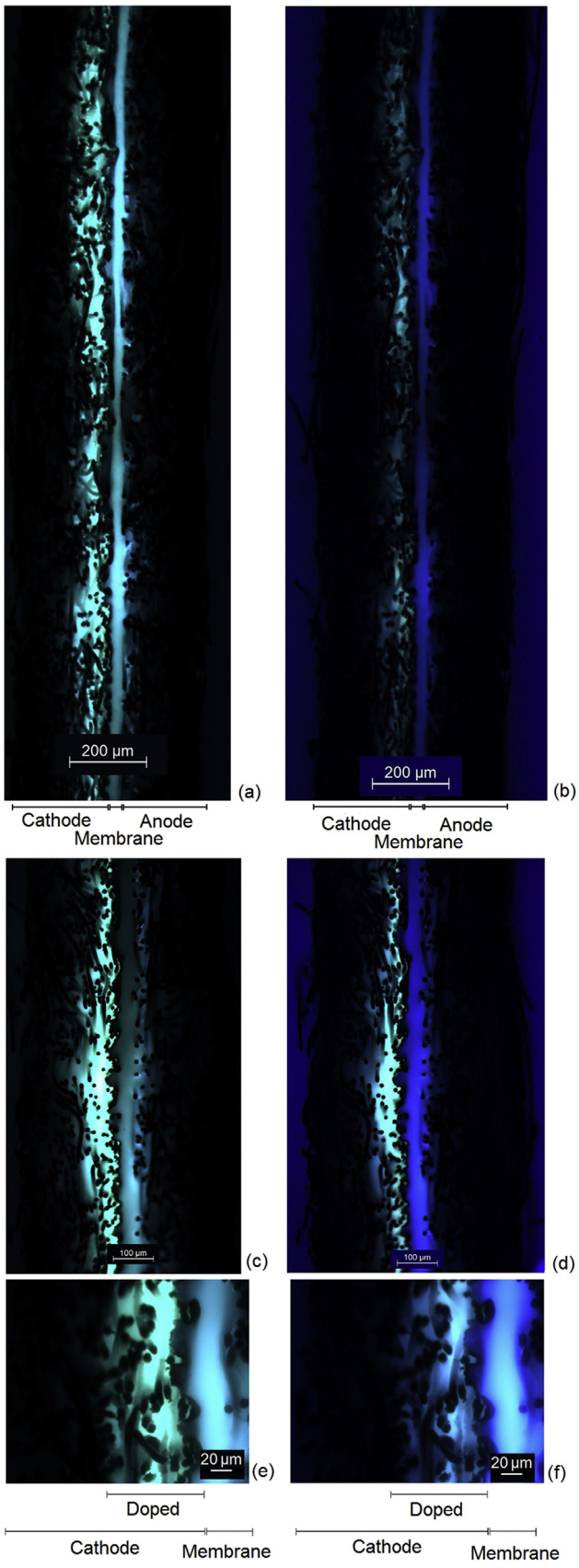

Fig. 5 – Comparison of unfiltered (left) and filtered (right) MEA cross sections at various magnifications (a) 100×, (b) 100× filtered, (c)200×, (d)200× filtered, (e)400×, (f)400× filtered.

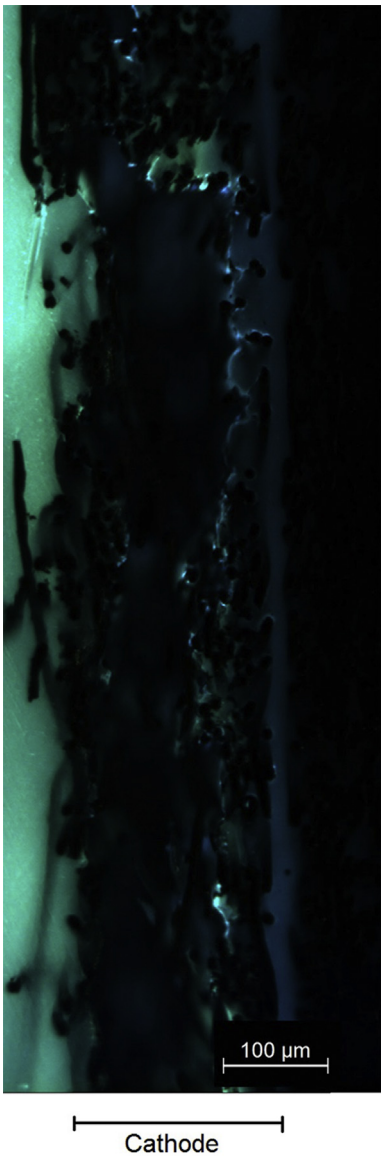

Fig. 6 – Observed 'bright region' on in MAC2 indicating delamination of membrane and GDM.

ink carrier solution, that can be imaged as the blue response. It is not possible to differentiate with any confidence the multiple sources of PTFE based autofluorescence.

The 1wt% EpoDye™ treated samples were able to produce a very strong fluorescence response immediately they were illuminated with a suitable ultra violet (UV) source. The illumination level does reduce the ability to identify specific fibers on the surface of the GDM, but the decreased image capture time makes this an attractive option.

The higher concentrations of fluorescent dye made no improvements to the images captured. Typically the MPL surface can be difficult to image with its characteristic 'black powder on black fiber' lack of contrast. Fig. 2(c) shows the active surface area of a 'proof of concept' test sample before MEA fabrication began. The fluorescence time is far less, and it is for this reason the texture of the fiber substrate in those

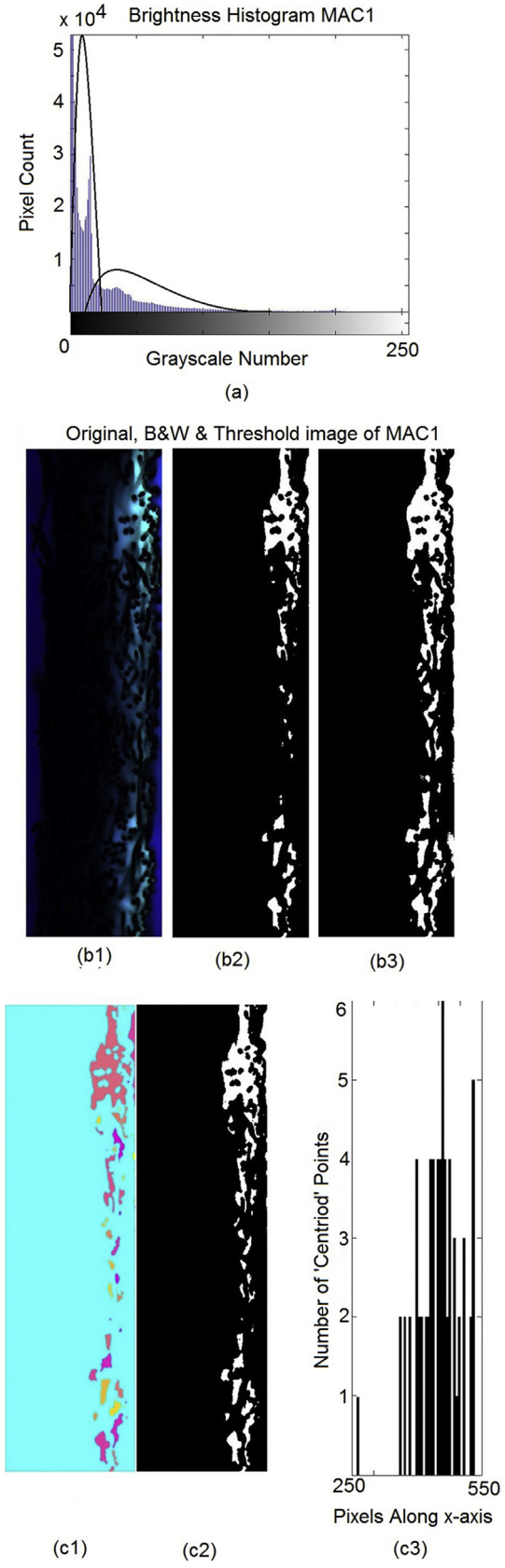

Fig. 7 – MAC1 Cathode image processing example (a) brightness histogram, (b1) filtered 200× fluorescent image, (b2) Black and white image transform, (b3) Otsuo image transform, (c1) PTFE region map for all particles, (c2) Otsuo transform, (c3) centroid point locations of individual particles in 'c2'.

areas not coated in catalyst ink is lost. This is the first time this type of image has been reported in a fuel cells context. The edge of the ink coated region is clearly visible, and there are notable features in the painted catalyst surface, with clear fissures in the surface of the active area leading deeper into the GDM. This test sample highlights the ability of this technique to quickly and easily asses the uniformity of catalyst coating for CCS fabrication procedures, and may prove useful in ink deposition optimization studies in the future. Once again we believe this is the first time it has been possible to distinguish PTFE added as part of the ink formulation on GDMs that have been pre-treated with a PTFE based hydrophobic coating.

The left hand images in Fig. 5 shows the standard response for a fluorescence doped MAC-MEA (left). It is immediately apparent that the characteristic 'blue' emission of the untreated PTFE is shifted to a green color, and also the characteristic 'yellow' response of the EpoDye™ is also shifted to the green as the two emitted frequencies 'mix'. By the addition an E4 filter the green response from the yellow EpoDye™ can be increased and the range of auto-fluorescence frequencies interfering with our understanding of the image can be limited. The ability to reduce the intensity of the response from the untreated PTFE in the Nafion® membrane, and the untreated hydrophobic coating of the GDM, greatly increases the contrast between phases, as can be seen in the right hand images in Fig. 5.

Applying this same approach at 100× magnification produces images that can be characterized digitally.

At this level it is still is possible to differentiate the segregation of PTFE layers in the GDM as a result of variable doping with EpoDye™ if additional image processing is used. At higher magnification still (400×) the flaring of the emitted light through the transparent mounting resin (used in the vacuum impregnation process) makes it impossible to differentiate between any PTFE based structures with confidence (Fig. 5 (e) and (f)).

The MAC 2 samples (where the MPL or 'CCS portion' of the ink is EpoDye™ loaded) again showed no significant variation in the emitted intensity response compared to those already studied. It is not possible to differentiate the order in which the fluorescent layers were painted on at any magnification 'by eye'. There is a degree of reflection and refraction through the doped PTFE, the un-doped hydrophobic coatings and the transparent epoxy resin mounting system vacuum impregnated into the GDM. It is possible that these light effects are causing difficulty in imaging the exact presence of the PTFE in the two separate ink layers. The depth of field may also be a factor. The depth of field of the images is clearly defined as follows for each magnification.

$$\frac{\lambda}{NA^2} = d_{field}(2) : \text{Depth of field}$$

Litster et al. [25] stated that the "... *observable range of the surface height ... is 30 μm ...*". Whilst our depths of field calculations are slightly less than theirs, we can reasonably expect

Table 2 – MAC1 PTFE region area (top) and centroid point location (bottom) along x-axis for MAC1 images.

Area per object	Section 1 (pixels)	Section 4 (pixels)	Section 5 (pixels)	Mean of means (μ)	StDev (σ)	(σ/μ)
Mean	7.61E+03	7.65E+03	7.82E+03	7.69E+03	1.10E+02	1.43%
Centroid 'x' coordinate	Section 1 (pixels)	Section 4 (pixels)	Section 5 (pixels)	Mean of means (μ)		
Mean	388	406	401	398.3	9.29	2.33%

to image fluorescent responses at a depth of 15 μm for the 50× magnification as our approaches are similar. However the washing out of the collected florescent light at high magnifications (and therefore reduced depth of field) indicate that emitted light from even further into the body of the sample than this assumed depth is being gathered. In order to overcome this limitation in the higher magnifications; several attempts were made at microtoming very thin slices of the MEA. Both the EpoFix™ epoxy mounting and standard epoxy filler mounting were extensively tested in this fashion but no specimens suitable for microscopy could be produced with the time and resources available. Therefore the technique of fluorescent doping, at its present stage of development, is only well suited to images that are in the 50 to 100 times magnification range.

One area observed in the fluorescence microscopy of the MAC 2 sample was notably different to the rest. In Fig. 6 there is a highly defined region with significantly increased emission. This 'lightening flash' may be a feature brought about by poor vacuum impregnation and represent light passing up through air gaps in the GDM. However the fact that the MAC2 sample gave such a very poor response when attempting to generate polarization curves gives rise to the far more likely possibility that this was a pre-existing defect in the MEA itself, and the fluorescent dye has congregated in the void space. In all probability this is a delamination effect (separation of the membrane and the catalyst/GDM layers from each other). It is unclear if the addition of the EpoDye™ is the cause of the delamination or not; but the reduced performance in both samples compared to the control sample could well be explained by a reduction in the adhesion of the various layers brought about by the addition of the fluorescent dye. If a more chemically compatible fluorescent dye, that does not reduce fuel cell performance, can be developed in the future; then there is an interesting possibility that this fluorescence microscopy method could be used for defect detection in MEA manufacturing techniques in the future.

Digital image analysis

Whilst it may not be possible to differentiate the layers separation visually, as can be seen in Fig. 7, the gathered data is amenable to image processing. Standard black and white conversion (Fig. 7 (b2)) leaves much to be desired. Setting the

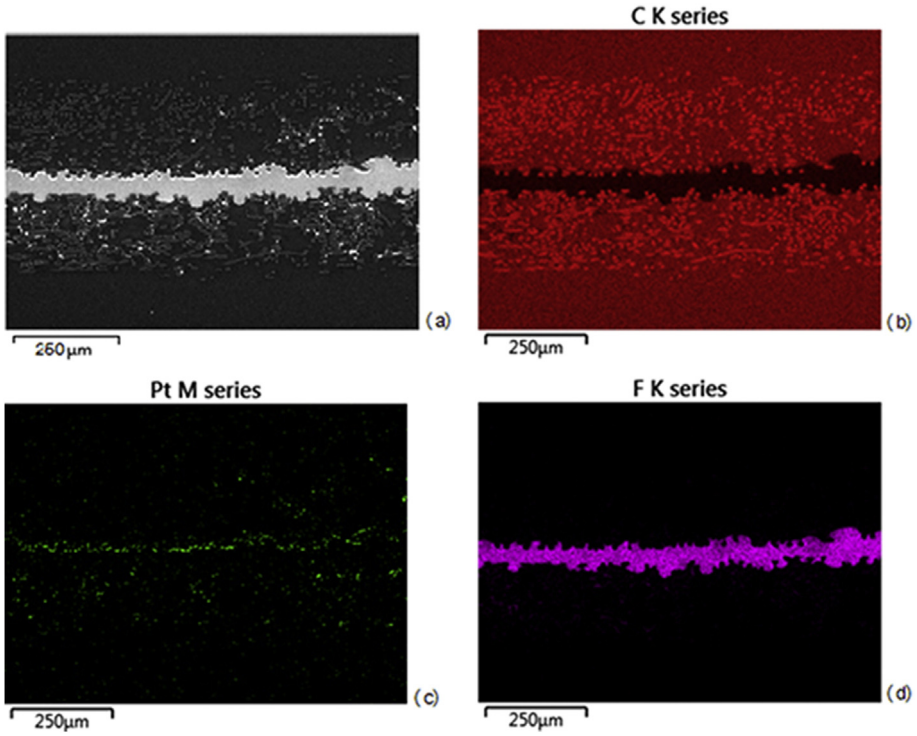

Fig. 8 – FEG-SEM of standard cathode GDM (a) FEG-SEM image, (b) back scatter carbon map, (c) back scatter platinum map, (d) back scatter fluorine map.

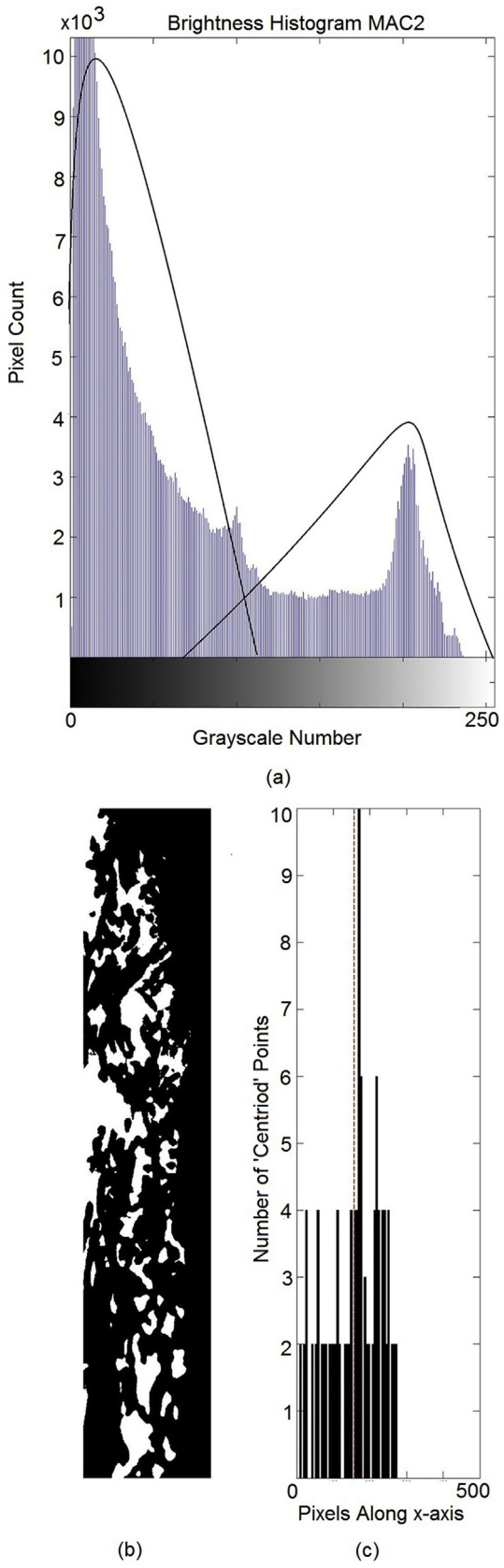

Fig. 9 – MAC2 Cathode image processing example (a) bimodal brightness histogram, (b) Otsuo transform, (c) centroid point of each particle distribution.

threshold at the mean point of all brightness in the original image results in the loss of too much information (Fig. 7(b2)), and so another method is required. The use of Otsu's method [34,35] (through the 'Graythresh' command in Matlab) shown in Fig. 7 (b3) does an acceptable conversion of the image for further analysis. For this approach to be valid the following assumptions must be true:

(i) Histograms (and therefore the image) are bi-modal
(ii) There is no relevant structure or geometry that needs to be specifically included
(iii) Illumination is uniform across the image and so bi-modality is a function of the time imaged and not a lighting effect

A bi-modal brightness distribution was achieved by cropping the field of view down to the point where only the Cathode GDM was largely visible (excluding as much of the Nafion membrane layer as was feasible). It is now possible to quantify the data (see Table 2). The 'graythresh' command in Matlab® automatically applies Otsuo's method to the selected image, and is applicable in this case. Fig. 7(a) assesses this, and whilst the bi-modal nature of the image could, ideally, be greater; it is strong enough that Otsu's method improves the number of PTFE regions in the GDM identified (as shown in Fig. 7 (b3)).

'Particle' identification

Having completed the converting of the image from the grayscale to black and white, the inbuilt image analysis functions in Matlab® can be used. It is simple to detect and quantify all the identified regions that are continuous with each other (the 'particle' effect) and those regions can be defined in several ways. Fig. 7(c1) shows the discretized 'continuous' regions as identified by the analysis parameters created from Otsu's Method.

As in all image analysis a certain degree of caution must be exercised when viewing the data, giving due consideration to the relative intensity for all possible test samples, lighting conditions and fluorescent responses. With care and practice the methodology can be applied with confidence of achieving consistent, repeatable results. Utilizing the inbuilt capabilities of the MatLab® program we can accurately return the area of all identified PTFE 'particle' or regions, their mean size, measure the perimeter of each particle or determine the 'centroid point' of each particle. As a measure of the distribution of the Nafion added into the GDM by the catalyst ink (or its MPL equivalent) the centroid point approach has been selected for this study.

Fig. 7 (c3) shows the histogram of doped PTFE regions and their position along the x axis of the image as defined by the centroid point.

In Fig. 7 (b2 and c2) we can see a region of depleted PTFE content approximately in the middle third of the image. This highlights the usefulness of this technique. Using this fluorescent methodology it is clear that we are failing to achieve a uniform distribution of PTFE based polymers in the CL (in the case the 'MAC1' test sample). In future work we could now optimize out catalyst deposition and MEA fabrication methods to reduce or eliminate the variation in the PTFE

Table 3 – MAC2 PTFE region Area (top) and Centroid Point location (bottom) along x-axis for MAC2 images.

Area per object	Section 3 (pixels)	Section 4 (pixels)	Section 7 (pixels)	Mean of means (μ)	StDev (σ)	(σ/μ)
Mean	5.97E+03	5.86+03	5.72 E+03	5.85E+03	1.27E+02	2.17%
Centroid 'x' coordinate	Section 1 (pixels)	Section 4 (pixels)	Section 5 (pixels)	Mean of means (μ)		
Mean	178	158	200	178.7	21.01	11.76%

component of the CL, and seek to optimize the performance of the MEA over time. Recall that Otsuo's method assigns pixels into one of two 'bins' and the automated thresholding procedure has excluded a significant amount of information from the original image in the central region of the image. The unprocessed image gave a false impression of a uniform PTFE distribution due to the refracted/reflected light traveling up through the transparent areas in the GDM. The automated image analysis now excludes light from the center of the image as it is not sufficiently bright to originate the within our depth of field study area (approx. 15 μm or less) surface of the sample.

Recall that in manufacturing sample 'MAC1', the non-doped MPL was applied directly to the GDM, and the doped CL was applied directly to the Membrane layer. The fluorescent dye has clearly moved away from the surface of the membrane. Utilizing a SEM (Fig. 8 was captured using a Leo (Carl Zeiss) 1530VP FEG-SEM (Germany) fitted with an Oxford Instruments X-Max 80 mm EDS detector (England) in the hope of improving PTFE image capture. As can be seen in Fig. 8 this did not prove to be the case.

Comparison to the PTFE distribution in Fig. 5 (d) and the processed images in Fig. 7, and the platinum distribution (Fig. 8 c) it is clear that the Pt has largely remained near the surface of the membrane, but that the PTFE suspension media of the catalyst ink has tracked up into the body of the GDM. It is equally clear that the EDX map for PTFE tracking in Fig. 8(d) has failed to identify this (the bright fluorine response from the Nafion membrane has 'swamped' the less bright fluorine response in other structures). The movement of the PTFE binder (with its dissolved fluorescent dye) up into the GDM fibers can only have happened at the time when the various parts of the MEA (MPL coated GDM and catalyzed membrane) were hot pressed together to form a single, fully adhered, unit. This is the first time it has been established that the PTFE component of a catalyst ink formulation can segregate away from the heavy metal component during MEA hot pressing. In the future it should be possible to utilize this fluorescent microscopy technique to optimize the MEA manufacturing technique and the degree of separation of Pt and PTFE required for optimum performance.

The addition of a small amount of platinum into the 'MPL' equivalent low concentration CL helps to map its distribution, and Fig. 8 (c) shows the MPL layer has penetrated a large way into the GDM (almost completely through in some places). Each pixel in the analyzed image space for the transformed images is 1.84 μm wide. In MAC 2, the (very low Pt concentration) 'MPL' applied to the GDM first was doped with the EpoDye™ and the subsequent CL applied to the membrane was not. A typical Otsuo transform and PTFE distribution for sample MAC2 is shown in Fig. 9. Table 3 shows a typical assessment of the PTFE regions within the GDM. The PTFE map using fluorescent microscopy and Otsuo's image analysis generates a similar depth of penetration. i.e. the both the PTFE and low concentration platinum 'tracker' have moved together through the GDM.

The layer thickness for CL and MPL, based on these results for the two separate MEAs can now be accurately determined as shown in Table 4. Note that in Fig. 10 the x plane represents the thickness of the GDM, with the value of '0' being the point furthest away from the membrane and the catalyst layer.

Conclusion and outlook

A new method for distinguishing the origin and location of PTFE in gas diffusion media as a result of catalyst ink or MPL applications is reported for the first time and report the following findings

a) It is possible to use Fluorescence microscopy to map the penetration of PTFE based products in the Catalyst Layer (CL) inks or Microporous layers (MPL) or applied to a substrate, and their penetration into the GDM itself.
b) The PTFE component of a catalyst ink formulation can track into the body of the GDM during the hot pressing stage of MEA manufacture.
c) Fluorescence based PTFE tracking is well suited to mapping the location of MPLs applied as a coated substrate directly to the GDE
d) The proposed system of fluorescence microscopy on Epo-Dye™ doped MEAs is accurate, with a low variance (less

Table 4 – Catalyst layer thickness estimation.

MAC1	Mean layer location (pixels)	Mean layer thickness (pixels)	Mean layer location along x (μm)	Standard error (μm)	Mean layer thickness (μm)	Standard error (μm)
Layer 1 (CL)	398.3	228.3	733	9.9	420	49.6
MAC 2	Mean layer location (pixels)	Mean layer thickness (pixels)	Mean layer location along x (μm)	Standard error (μm)	Mean layer thickness (μm)	Standard error (μm)
Layer 2 (MPL)	178.7	316.7	329	22.4	583	52.7

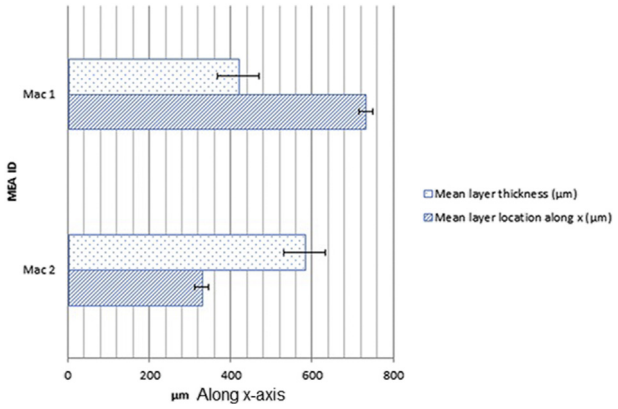

Fig. 10 – Mean centroid location and mean layer thickness comparison for MAC1 (CL) and MAC2 (MPL).

than 12% of the measured value in any image captured; typically much less) and distinct separation between the standard errors for each region (380 µm between mean locations of individual layers in the GDM).

e) The total area of the two samples ('MAC1' a Membrane Coated layer and 'MAC2' a GDM coated layer) shows a similar degree of separation – with the 'Fluorescent CL layer' (MAC1) having the largest area of the two samples

This is the first time it has been possible to differentiate between the likely distributions of PTFE in the GDM added as a result of catalyst ink or MPL applications and subsequent manufacturing processes. Whilst the distribution of some atomically heavier materials in the GDM can be tracked through X-ray techniques, these methods cannot distinguish between carbon structures. It has been until now difficult to differentiate with certainty between fibers and the binder agents present. . Fluorine mapping using scanning electron microscopy techniques such as EDX to map fluorine distribution ineffective. It cannot reliably differentiate between different sources of PTFE present in the GDM (e.g. those found in Nafion, CL ink, MPL binder or hydrophobic coating on GDM fibers).

The use of common digital analyses techniques, such as Otsu's method, utilized in the Matlab® command 'graythresh', is effective and produces quantifiable results that are of use in a research context when combined with fluorescence microscopy. The depth of field for the fluorescence images generated means the technique is best suited to cross sectional images of MEAs in the 50 to 100 times magnification range.

Further developments in the compatibility of fluorescent dyes with PTFE based binder agents for use in PEMFCs, so that the PEMFC can work normally, is required. This would be a significant body of work, that would make possible direct observation of degradation effects on PTFE based structures in the GDM over its working life. If several different frequency responses could be developed (i.e. different colored fluorescent dyes that do not negatively impact the performance the completed MEA), individual PTFE structures such as the hydrophobic coating, the MPL and the binder agents for the CL could all be analyzed separately in a single MEA. Their contribution to losses in performance over time could then be calculated directly and optimization of fuel cell performance could be advanced.

Acknowledgments

The technical support from Mr. Shawn Fowler and Dr Keith Yendall (Department of Materials, Loughborough University) was crucial to the successful completion of this work.

This work could not have been completed without the help and support of the EPSRC through its funding of the Doctorial training Centre (DTC) for Hydrogen, Fuels Cells and Their Applications at the University of Birmingham (EPSRC Grant EP/G037116/1), and also the FUTURE vehicles project (EPSRC Grant EP/I038586/1). The supporting research data for this article can be found at http://dx.doi.org/10.17028/rd.lboro.3562128.v1.

Nomenclature

T	threshold brightness
W	Brightness intensity 'weighting'
n	A number (of pixels)

Greek

μ	mean value
σ^2	variance

Subscripts

b	background
f	foreground

REFERENCES

[1] Lim C, Wang CY. Effects of hydrophobic polymer content in GDL on power performance of a PEM fuel cell. Electrochim Acta 2004;49:4149–56.

[2] Hiramitsu Y, Sato H, Kobayashi K, Hori M. Controlling gas diffusion layer oxidation by homogeneous hydrophobic coating for polymer electrolyte fuel cells. J Power Sources 2011;196:5453–69.

[3] Hiramitsu Y, Kobayashi K, Hori M. Gas diffusion layer design focusing on the structure of the contact face with catalyst layer against water flooding in polymer electrolyte fuel cell. J Power Sources 2010;195:7559–67.

[4] Chapuis O, Prat M, Quintard M, Chane-Kane E, Guillot O, Mayer N. Two-phase flow and evaporation in model fibrous media application to the gas diffusion layer of PEM fuel cells. J Power Sources 2008;178:68.

[5] Lin G, Nguyen TV. Effect of thickness and hydrophobic polymer content of the gas diffusion layer on electrode flooding level in a PEMFC. J Electrochem Soc 2005;152:A1942–8.

[6] Park S, Lee J, Popov BN. A review of gas diffusion layer in PEM fuel cells: materials and designs. Int J Hydrogen Energy 2012;37:5850–65.

[7] Park J, Oh H, Ha T, Lee YI, Min K. A review of the gas diffusion layer in proton exchange membrane fuel cells: durability and degradation. Appl Energy 2015;155:866–80.

[8] Weng F, Hsu C, Li C. Experimental investigation of PEM fuel cell aging under current cycling using segmented fuel cell. Int J Hydrogen Energy 2010;35:3664–75.

[9] Tang W, Lin R, Weng Y, Zhang J, Ma J. The effects of operating temperature on current density distribution and impedance spectroscopy by segmented fuel cell. Int J Hydrogen Energy 2013;38:10985–91.
[10] Lin R, Cao C, Ma J, Gülzow E, Andreas Friedrich K. Optimizing the relative humidity to improve the stability of a proton exchange membrane by segmented fuel cell technology. Int J Hydrogen Energy 2012;37:3373–81.
[11] Wang Y, Chen KS. Effect of spatially-varying GDL properties and land compression on water distribution in PEM fuel cells. J Electrochem Soc 2011;158:B1292–9.
[12] Wang Y, Feng X. Analysis of the reaction rates in the cathode electrode of polymer electrolyte fuel Cells: II. Dual-Layer electrodes. J Electrochem Soc 2009;156:B403–9.
[13] Feng X, Wang Y. Multi-layer configuration for the cathode electrode of polymer electrolyte fuel cell. Electrochim Acta 2010;55:4579–86.
[14] Newbury DE, Ritchie NWM. Elemental mapping of microstructures by scanning electron microscopy-energy dispersive X-ray spectrometry (SEM-EDS): extraordinary advances with the silicon drift detector (SDD). J Anal At Spectrom 2013:973–88.
[15] Antoine O, Bultel Y, Ozil P, Durand R. Catalyst gradient for cathode active layer of proton exchange membrane fuel cell. Electrochim Acta 2000;45:4493–500.
[16] Xie Z, Navessin T, Shi K, Chow R, Wang Q, Song D, et al. Functionally graded cathode catalyst layers for polymer electrolyte fuel cells: II. Experimental study of the effect of nafion distribution. J Electrochem Soc 2005;152:A1171–9.
[17] Wang Q, Eikerling M, Song D, Liu Z, Navessin T, Xie Z, et al. Functionally graded cathode catalyst layers for polymer electrolyte fuel cells: I. Theoretical modeling. J Electrochem Soc 2004;151:A950–7.
[18] Song D, Wang Q, Liu Z, Eikerling M, Xie Z, Navessin T, et al. A method for optimizing distributions of Nafion and Pt in cathode catalyst layers of PEM fuel cells. Electrochim Acta 2005;50:3347–58.
[19] Rama P, Liu Y, Chen R, Ostadi H, Jiang K, Zhang X, et al. An X-ray tomography based lattice Boltzmann simulation study on gas diffusion layers of polymer electrolyte fuel cells. J Fuel Cell Sci Technol 2010;7. 031015–031015.
[20] Gao Y, Zhang X, Rama P, Chen R, Ostadi H, Jiang K. Lattice Boltzmann simulation of water and gas flow in porous gas diffusion layers in fuel cells reconstructed from micro-tomography. Comput Math Appl 2013;65:891–900.
[21] Manke I, Hartnig C, Grünerbel M, Lehnert W, Kardjilov N, Haibel A, et al. Investigation of water evolution and transport in fuel cells with high resolution synchrotron x-ray radiography. Appl Phys Lett 2007;90:174105.
[22] Zhang J, Kramer D, Shimoi R, Ono Y, Lehmann E, Wokaun A, et al. In situ diagnostic of two-phase flow phenomena in polymer electrolyte fuel cells by neutron imaging: part B. Material variations. Electrochim Acta 2006;51:2715–27.
[23] Tötzke C, Gaiselmann G, Osenberg M, Bohner J, Arlt T, Markötter H, et al. Three-dimensional study of compressed gas diffusion layers using synchrotron X-ray imaging. J Power Sources 2014;253:123–31.
[24] Lee J, Hinebaugh J, Bazylak A. Synchrotron X-ray radiographic investigations of liquid water transport behavior in a PEMFC with MPL-coated GDLs. J Power Sources 2013;227:123–30.
[25] Litster S, Sinton D, Djilali N. Ex situ visualization of liquid water transport in PEM fuel cell gas diffusion layers. J Power Sources 2006;154:95–105.
[26] Cropotova J, Tylewicz U, Cocci E, Romani S, Dalla Rosa M. A novel fluorescence microscopy approach to estimate quality loss of stored fruit fillings as a result of browning. Food Chem 2016;194:175–83.
[27] Le Duigou A, Kervoelen A, Le Grand A, Nardin M, Baley C. Interfacial properties of flax fibre–epoxy resin systems: existence of a complex interphase. Compos Sci Technol 2014;100:152–7.
[28] Wittmann JC, Meyer S, Damman P, Dosière M, Schmidt H. Preparation and characterization of side-chain liquid crystalline polymer thin films aligned on PTFE friction-transferred layers. Polymer 1998;39:3545–50.
[29] Takahashi I, Kocha SS. Examination of the activity and durability of PEMFC catalysts in liquid electrolytes. J Power Sources 2010;195:6312–22.
[30] Frey T, Linardi M. Effects of membrane electrode assembly preparation on the polymer electrolyte membrane fuel cell performance. Electrochim Acta 2004;50:99–105.
[31] Marquis J, Coppens M-. Achieving ultra-high platinum utilization via optimization of PEM fuel cell cathode catalyst layer microstructure. Chem Eng Sci 2013;102:151–62.
[32] Gerteisen D, Zamel N, Sadeler C, Geiger F, Ludwig V, Hebling C. Effect of operating conditions on current density distribution and high frequency resistance in a segmented PEM fuel cell. Int J Hydrogen Energy 2012;37:7736–44.
[33] Ploem JS, Walter F. Multi-wavelength Epi-illumination in fluorescence microscopy, 2015. 2001.
[34] Otsu N. A threshold selection method from gray-level histograms, systems, man and cybernetics. IEEE Trans 1979;9:62–6.
[35] Greensted A. Otsu thresholding, 2015. 2010.